Bloch-Surface-Waves-Induced Fano Resonance in Magneto-Optical Response of Magnetophotonic Crystals

I.V. Soboleva, M.N. Romodina, K.A. Korzun, A.I. Musorin, and A.A. Fedyanin

Faculty of Physics, Lomonosov Moscow State University, Moscow 119991, Russia

ABSTRACT

Magnetophotonic crystals (MPCs) support Bloch surface waves (BSWs) and waveguided modes (WGMs) propagation. The influence of the BSW on the Faraday effect in the one-dimensional MPCs is studied. The technique of measuring the angle of Faraday rotation in the MPCs in attenuated total internal reflection scheme in Kretschmann configuration is discussed. The spectra of Faraday rotation demonstrate a Fano-shaped resonance near the spectral-angular position of the BSW resonance both for *s*- and *p*-polarized incident light. The presence of the feature in the spectrum of *p*-polarized light can be explained by the Faraday rotation effect and subsequent BSW excitation mutually enhancing each other.

Keywords: Faraday effect, surface electromagnetic waves, magnetophotonic crystals, Kretschmann configuration

1. INTRODUCTION

In recent decades nanophotonics has focused on the search of the effective ways to control the light on the microscale. The ability of magneto-optical effects to control the polarization of the light beam led to a renewal of interest in them. For example, recently it was shown that the magneto-optical effects such as Faraday and Kerr effects can be used to achieve the polarization shaping of ultrashort laser pulse.[1] Ultrashort pulse shaping is required in the coherent control of quantum states,[2–4] plasma dynamics[5] and other important applications.[6–8] The Faraday effect is governed by a spin-orbit interaction and manifests itself as a rotation of the polarization plane of linearly polarized light passing through the magnetic material. The angle of rotation is determined by the velocity disparity between the left and right circularly polarized waves and the light optical path length in the magnetic medium. In nanostructures with narrow resonances in the reflectance spectra, for example, magnetophotonic crystals,[9–11] microcavities[12–15] or magnetoplasmonic gratings,[16,17] the Faraday effect can be significantly enhanced due to the phase shifts across the resonance.[18]

This work is devoted to the influence of Bloch surface waves in one-dimensional magnetophotonic crystals (MPCs) on the spectral dependence of the Faraday rotation angle. The MPCs are the microstructures consisting of layers of magnetic and non-magnetic materials[19] where the excitation of surface states has recently been shown.[20] Bloch surface waves (BSWs) are excited at the interface of two dielectrics,[21,22] in this case, the MPC and air, and have an extremely high mean free path and very low spectral and angular width of the resonance.[23,24] The dispersion relation of the BSWs in photonic crystals lie behind the light line and their excitation requires special excitation schemes.[25] Attenuated total internal reflection schemes in Otto and Kretschmann-Raether geometries are effective, however, the magneto-optical measurement technique requires the due regard of the prism.[26] This paper describes the correct algorithm to measure the Faraday effect near resonance of BSW excited in the MPC with the attenuated total internal reflection scheme in the Kretschmann geometry. The Faraday-rotation-angle spectra are experimentally obtained in the MPC simultaneously with the BSW excitation. The results are discussed taking into account the numerical and experimental reflectance spectra of magnetophotonic crystal.

I.V.Soboleva also at: Frumkin Institute of Physical Chemistry and Electrochemistry, Russian Academy of Sciences, Moscow 119071, Russia

Contact authors through the Lab website http://nanolab.phys.msu.ru

Photonic and Phononic Properties of Engineered Nanostructures VII, edited by Ali Adibi, Shawn-Yu Lin, Axel Scherer, Proc. of SPIE Vol. 10112, 1011210 · © 2017 SPIE
CCC code: 0277-786X/17/$18 · doi: 10.1117/12.2252852

2. SAMPLES

The studied MPC sample consists of 7 bilayers of Ta_2O_5 and SiO_2 with thickneses of 97 nm and 138 nm, respectively, topped with a layer of Bi-substituted yttrium-iron-garnet (Bi:YIG) with thickness of 1055 nm. The sample was fabricated by layer-by layer ion-beam sputtering onto a quartz substrate and annealed for 15 minutes at a temperature of 750°C. The center of photonic band gap at normal incidence of light is supposed to be at the wavelength of 810 nm.

The numerical calculations of the reflectance versus incidence angle and wavelength were made using the Berreman's 4x4 matrix method[27,28] for the sample in the Kretschmann configuration of the attenuated total internal reflection scheme.[29] The dielectric permittivity tensor can be represented in the following form

$$\varepsilon = \begin{pmatrix} \varepsilon & -ig & 0 \\ ig & \varepsilon & 0 \\ 0 & 0 & \varepsilon \end{pmatrix},$$

where ε is the electric permittivity of the medium, and g describes the magnetization-induced gyration of the material with a magnetization normal to the MPC surface. The real and imaginary components of the dielectric permittivity as a function of the light wavelength for Ta_2O_5, SiO_2 and Bi:YIG were taken from optical measurements and magnetic field is introduced by choosing $g = 0.0045$ for Bi:YIG.

The MPC reflectance versus the angle of incidence and wavelength for s- and p-polarized light are shown in Fig. 1. A clear light line appears at the angle of total internal reflection being equal to 43.6^0 for the quartz/air

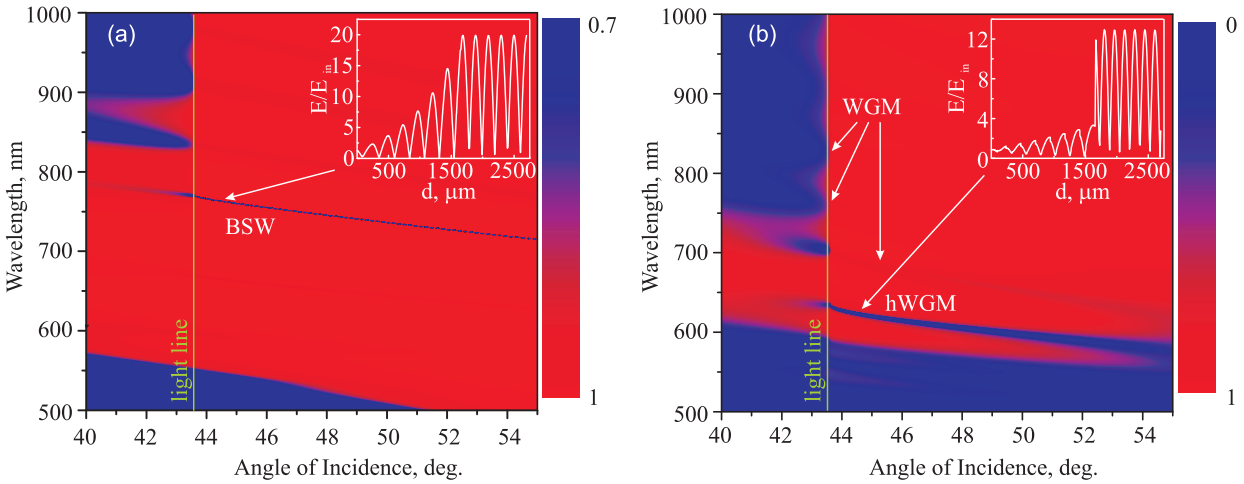

Figure 1. (a) The MPC reflectance versus the angle of incidence and wavelength of s-polarized light. Inset: Distribution of the s-polarized electric field with the wavelength of 762 nm among the MPC layers. (b) The MPC reflectance versus the angle of incidence and wavelength of p-polarized light. Inset: Distribution of the p-polarized electric field with the wavelength of 622 nm among the MPC layers.

interface. For higher incident angles a number of minima appear in reflectance spectra for both polarizations of light. A narrow minimum inside the PBG is observed in reflectance specrtum for s-polarized incident light (Fig.1a). This minimum is located at 770 nm for incidence angle equal to 43.6^0 and move toward the smaller wavelengths with increase of incident angle. There are also two wide minima in reflectance spectrum of p-polarized light (Fig.1b) at 700 nm and 630 nm for the incidence angle of total internal reflection, and two more minima located outside the first PBG and starting from 784 nm and 820 nm at the angle of total internal reflection.

An electric field distribution within the sample was calculated for the angle of incidence equal to 44.5^0 at wavelengths of the minima in reflectance spectra. The distribution of the electric field at the wavelength of 622 nm, which corresponds to the deepest minimum in reflectance spectrum of p-polarized light, is shown in inset of Fig.1b. The field is evenly distributed within the top layer and is almost absent inside the MPC. This

electric field distribution allows us to consider this mode as hybrid surface waveguided mode (hWGM) of the MPC. Other three detectable minima in calculated reflectance spectra correspond to the electric-field maximum in the central layers and its decrease to the MPC edges. These field distributions are typical for the normal waveguided modes (WGM) of the MPC. The distribution of the electric field at wavelength of 762 nm for the *s*-polarized incident light is shown in the inset of Fig.1a. Exponential decrease of the electric field within the MPC corresponds to the BSW excitation in the MPC structure.

The MPC sample optical and magneto-optical properties were characterized using transmittance spectroscopy in stationary magnetic field directed normal to the sample surface. The magnetic field strength was enough to saturate the MPC sample. Reflectance spectra and Faraday rotation spectra measured at normal incidence of light are shown in Fig. 2. The MPC photonic band gap is centered at wavelength of 820 nm. Two minima

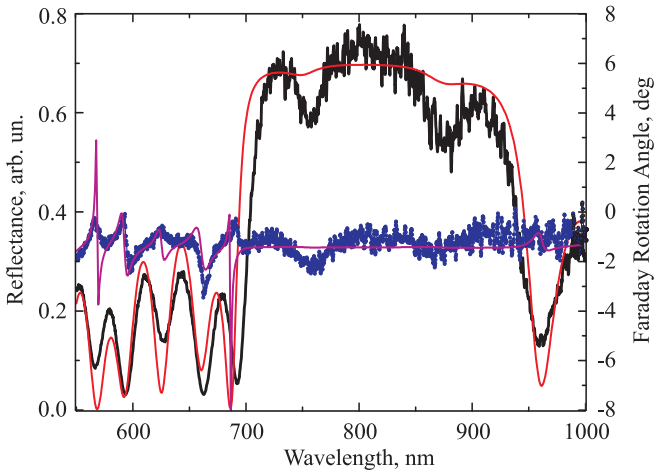

Figure 2. Experimental and calculated spectra of reflectance (black and red curves) and Faraday rotation angle (blue and magenta curves), respectively.

occur within the photonic band gap spectral range of reflectance spectra corresponding to light localized state in the top layer. There are some peculiarities in Faraday rotation corresponding to the oscillations in reflectance spectra which was previously observed in similar structures due to multipass traveling of light through the layered structure. The calculation results are in good agreement with the experimental data.

3. EXPERIMENTAL RESULTS AND DISCUSSION

The experimental setup to study the BSW-induced magneto-optical effects is shown in Fig. 3. The halogen lamp (1) is used as a source. Collimator consisting of confocal converging lenses (2) and (4) and diaphragms (3) and (5) forms a white-light beam with angle aperture close to 1^0. GlanTaylor prism (6) is used as polariser to control the polarization of the incident light. The MPC sample (8) was placed on the BK7-glass right-angle prism (7) providing the coupling beyond the light line at the glass/air interface. Immersion oil provided a contact between the sample and the prism. The magnet (9) was placed face to face with the back side of the sample to create a stationary magnetic field with strength about 2.7 kOe and directed perpendicular of MPC sample surface. The magnetic field strength was enough to saturate the MPC sample. The sample junction and a detector arm were placed on goniometer stage allowing a matched $\theta - 2\theta$ rotation. After reflecting from the sample the beam passed the another GlanTaylor prism (10) used as an analyzer, collected into the optical fiber (11) and detected by the spectrometer (12). Reflectance spectra of *s*- and *p*-polarized light were measured for different angles of incidence. All spectra were obtained for angles behind the light line. Besides, the Faraday rotation angle spectra were obtained. For this purpose reflectance spectra were measured for analyzer rotation angles varied from 0^0 to 360^0 with step of 1^0. The dependencies of reflectance R on the angle of analyzer rotation φ were fitted with the Malus's law $R(\varphi) = R_0 \cos^2(\varphi + \varphi_0)$ for each wavelength, where constant φ_0 is determined by the angle between the incident and reflected light polarization directions. Dependences $\varphi_0(\lambda)$ were obtained for the opposite directions of magnetic field as $\varphi_+(\lambda), \varphi_-(\lambda)$. Faraday rotation angle φ_F was taken as a half of Malus's

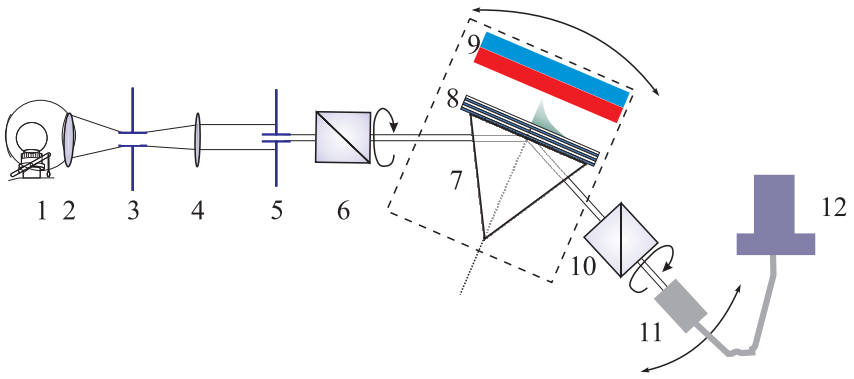

Figure 3. Sketch of the experimental setup.

law phase difference for opposite directions of the magnetic field $\varphi_F(\lambda) = (\varphi_+(\lambda) - \varphi_-(\lambda))/2$. These allows us to obtain the spectra of the magneto-induced polarization plane rotation angle for each angle of light incidence.

Reflectance spectra and spectra of Faraday rotation angle for *s*- and *p*-polarized light were obtained for incidence angles from 42^0 to 53.7^0. Hereinafter, the angle of incidence is given for light goes inside the prism to the MPC sample substrate. Angle of total internal reflection equals to 41.1^0 for the prism / air interface. Typical spectra are presented in Fig. 4. Reflectance spectra of *s*-polarized light demostrate two deep minima. The blue

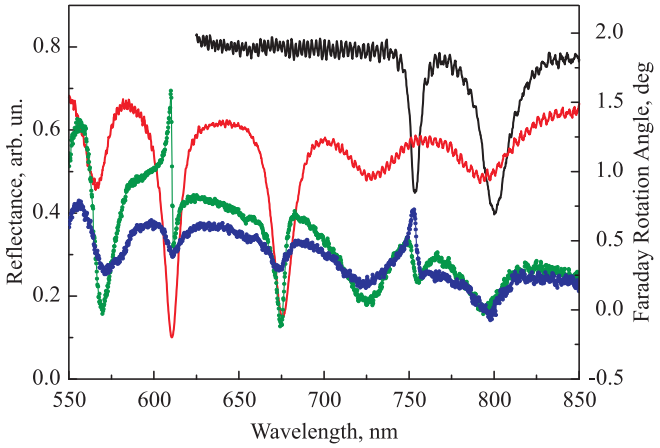

Figure 4. Experimental spectra of reflectance (black and red curves) and Faraday rotation angle (blue and green curves) measured for *s*- and *p*-polarization of the incident light, respectively. Angle of incidence is 43.3^0.

one corresponds to the BSW resonance and the red one is caused by the waveguided mode excitation. At the reflectance spectra of *p*-polarized light there is a number of minima. According to calculations, we consider the minimum at wavelength of 610 nm relating to the hWGM resonance and all other ones as the normal WGM modes of the MPC. All the features shift to shorter wavelenghts as incidence angle increases. Minima corresponding to the WGMs in reflectance spectrum of *p*-polarized light almost disappear at incidence angle of 53.7^0 because of the Brewster effect at the Ta_2O_5 / SiO_2 interfaces.

The spectra of Faraday rotation angle demonstrate features which spectral positions correspond to those in the reflectance spectra. Features at wavelengths of 610 and 750 nm have the Fano-shaped spectral line. The resonances relate to the excitation of the surface modes, which electric-field distributions are shown in the insets of the Fig. 1. The spectral positions of the normal WGMs correspond to the symmetric-shape minima appearing at the spectra of Faraday rotation angle.

Despite the fact that the calculation results are in a good agreement with the experimental data of the reflectance spectroscopy, they poorly describe the spectra of the Faraday rotation angle. The numerical spectra of Faraday rotation angle are presented in Fig. 5a. The calculations are performed for the incident angle of

43.3^0. The corresponding experimental data are shown for comparison. There are the features in calculated and

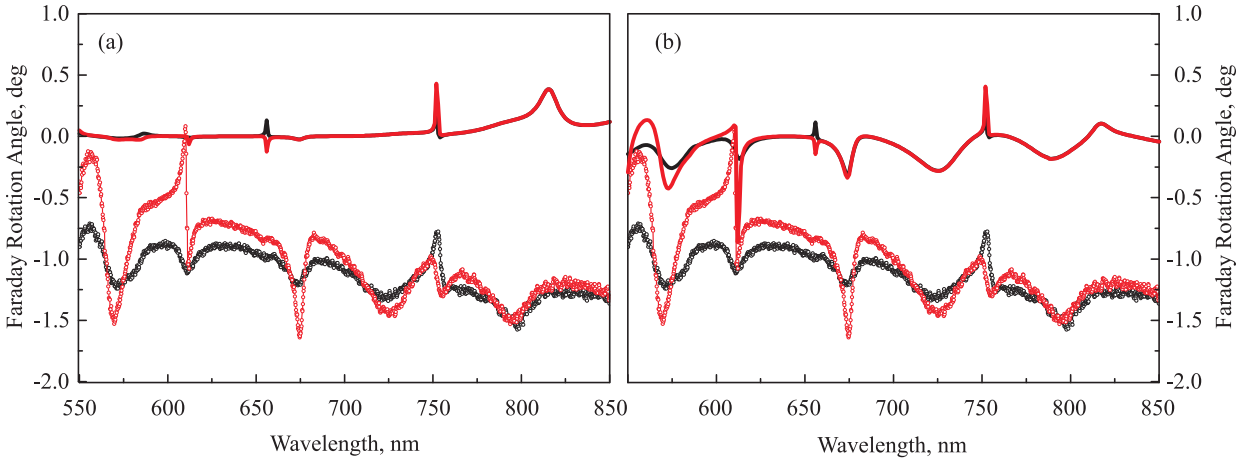

Figure 5. Calculated (lines) and experimental (dots) spectra of Faraday rotation angle for *s*- (black curves) and *p*-polarized (red curves) light. Experimental curves are displaced by -1.5^0 for clarity, the numerical scale is only correct for the calculated spectra. (a) Spectra are calculated for pure *s*- and *p*-polarization of the incident light. (b) Spectra are calculated for incident polarization that are linear but differ from the pure *s*- and *p*-polarization by 0.15^0.

experimental spectra of Faraday rotation angle at the same wavelengths, for example, of 569 nm, 611 nm, 675 nm, 754 nm. But features with spectral positions of 726 nm and 795 nm observed in the experiment are missed in the calculated spectra. We tried to make calculations for the case when the MPC sample is illuminated with the light being linearly polarized but its polarization is differ from true *s*- or *p*-polarization. The calculations were made for superposition of *s*- and *p*-polarized light. The difference from *s*-polarization was chosen to be equal to 0.15^0. The results are shown in Fig. 5b. In this case amplitudes of minima in the Faraday rotation angle spectra become bigger and features appear at wavelenghts of 726 nm and 795 nm. Such behavior is connected with different reflection of *s*- and *p*-polarized light from each boundary of the sample that leads to the nonmagnetic contribution in polarization plane rotation. These calculation results give the better agreement with the experimental data. It can be concluded that the experimentally obtained spectra of the Faraday rotation angle contain additional impacts made not by the sample and significantly influence the form of the spectra.

It has previously been shown[26] that the Faraday effect can also be observed in prism made from the BK7 glass when magnetic field is applied. Although glass is a diamagnet and its magnetic susceptibility is negligible, the optical path of light inside the prism is of many orders of magnitude greater than in the sample magnetic layer and Faraday effect in the prism can reach the detectable values. It is crucial for study of the magneto-optical effects in the MPC using Kretschmann scheme, since even a slight deviation of the incident light polarization from *s* and *p* leads to a significant distortion of the spectrum of the angle of rotation of the polarization plane in the MPC. Moreover, the Faraday effect in the prism depends on the direction of magnetic field and measurement technique described above can not take it into account properly. The following algorithm is used for measuring the true spectrum of the Faraday rotation in the MPC sample. First, the method described above was used to measure the value of the Faraday effect in the prism. Then polarizer was rotated from the position corresponding to *s*- or *p*-polarization to compensate for this effect and achieve true *s*- or *p*-polarization of light incident from the prism to the MPC sample. Further measurements were performed as previously described. The obtained result was adjusted to half of the measured value of the Faraday effect in the prism to take into account the Faraday rotation of the polarization of light reflected from the sample. The result corresponds to the spectrum of the Faraday rotation in the MPC sample. Fig. 6 demonstrates the spectra of Faraday rotation measured with and without correction for the Faraday effect in the prism. For the correction polarizer was turned from *s*- and *p*-polarizations positions for 0.35^0 in different directions for opposite directions of magnetic field. Spectra of Faraday rotation angle after using the correction algorithm became more gentle, moreover, some features, corresponding to the WGMs in reflectance spectra, disappeared. The new experimental spectra are much better correlated with the numerical results.

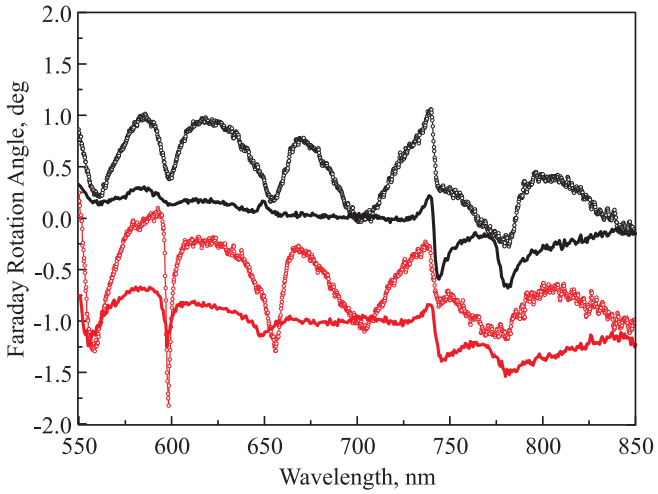

Figure 6. Spectra of Faraday rotation angle for s- (black curves) and p-polarized (red curves) light, measured with (solid curves) and with no correction (open dots) for the Faraday rotation inside the prism. Curves corresponded to the p-polarized light are displaced by -1^0 for clarity, the numerical scale is only correct for the s-polarized light. Incident angle is 45^0.

Finally, the spectra of the Faraday rotation of s- and p-polarized light is presented in Fig. 7. Features corresponded to the resonances of the BSW, hWGM and WGM modes of the MPC are observed in the spectra. Now the BSW observed at the wavelength of 740 nm is evident to cause the largest modification of the Faraday rotation spectra that corresponds to the numerical results. Fano shape of the resonance is observed both for s- and p-polarizations of the incident light. The presence of the feature in the spectrum of p-polarized light at

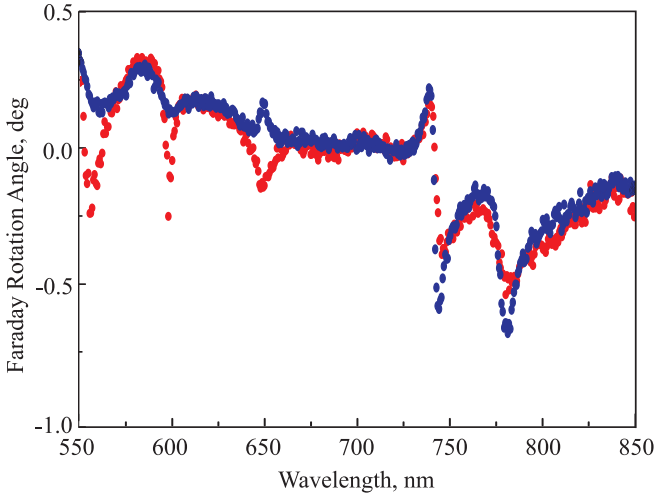

Figure 7. Experimental spectra of the Faraday rotation angle in the MPC of s- (red curve) and p-polarized light.

the wavelenght, corresponding to the BSW in s-polarized light, can be explained by the rotation of polarization plane as magnetic field is applied. Subsequent BSW's excitation leads to further Faraday rotation and these two phenomena mutually enhance each other. Fano shape of the resonance in Faraday rotation spectra is observed due to the spectral proximity of the s-polarized BSW and p-polarized WGM resonances. The phase of the reflected light varies as a function of light wavelength in the vicinity of any resonance; moreover, the phase change is slow near the resonance with a low Q-factor and exhibits a sharp jump near the resonance with a high Q-factor resonances. In this case the BSW and WGM resonances can be considered as being of the high and low Q-factor, respectively. The difference in the phase changes in s- and p-polarized light leads to the polarization rotation of the resultant reflected wave and causes the enhancement and change in sign of the Faraday rotation.

A similar mechanism for Faraday rotation with changing sign was described for the surface plasmon resonance in magnetoplasmonic structures[18,30] and numerically predicted for the BSW in the MPC.[29]

4. CONCLUSIONS

In this paper the influence of the Bloch surface waves on the Faraday effect in one-dimensional magnetophotonic crystals is studied. The method of measuring the angle of Faraday rotation in magnetophotonic crystals in attenuated total internal reflection scheme in Kretschmann configuration is discussed. The excitation of the Bloch surface waves are experimentally and numerically observed in the magnetophotonic crystal. The spectra of Faraday rotation demonstrate a Fano-shaped resonance near the spectral-angular position of the Bloch surface wave resonance both for *s*- and *p*-polarized incident light. The presence of the feature in the spectrum of *p*-polarized light can be explained by the Faraday rotation effect and subsequent BSW excitation mutually enhancing each other.

ACKNOWLEDGMENTS

This work was partially supported by the Russian Ministry of Education and Science (#14.W03.31.0008) and the Russian Foundation for Basic Research.

REFERENCES

[1] Rahimi, E. and Sendur, K. *J. Opt. Soc. Am. B* **33**, A1 (2016).
[2] Press, D., Ladd, T. D., Zhang, B., and Yamamoto, Y. *Nature (London)* **456**, 218 (2008).
[3] Brixner, T., Krampert, G., Pfeifer, T., Selle, R., Gerber, G., Wollenhaupt, M., Graefe, O., Horn, C., Liese, D., and Baumert, T. *Phys. Rev. Lett.* **92**, 208301 (2004).
[4] Warren, W. S., Rabitz, H., and Dahleh, M. *Science* **259**, 1581 (1993).
[5] He, Z.-H., Hou, B., Lebailly, V., Nees, J. A., Krushelnick, K., and Thomas, A. G. R. *Nat. Commun.* **6**, 7156 (2015).
[6] Assion, A., Baumert, T., Bergt, M., Brixner, T., Kiefer, B., Seyfried, V., Strehle, M., and Gerber, G. *Science* **282**, 919 (1998).
[7] Ren, X., Makhija, V., and Kumarappan, V. *Phys. Rev. Lett.* **112**, 173602 (2014).
[8] Xie, X., Dai, J., and Zhang, X.-C. *Phys. Rev. Lett.* **96**, 075005 (2006).
[9] Zhdanov, A., Fedyanin, A., Aktsipetrov, O., Kobayashi, D., Uchida, H., and Inoue, M. *J. Magn. Magn. Mater.* **300**, e253 (2006).
[10] Khanikaev, A., Baryshev, A., Lim, P., Uchida, H., Inoue, M., Zhdanov, A., Fedyanin, A., Maydykovskiy, A., and Aktsipetrov, O. *Phys. Rev. B* **78**, 193102 (2008).
[11] Murai, S., Yao, S., Nakamura, T., Kawamoto, T., Fujita, K., Yano, K., and Tanaka, K. *Appl. Phys. Lett.* **101**, 151121 (2012).
[12] Steel, M. J., Levy, M., and Osgood, R. M. *J. Lightwave Technol.* **18**, 1297 (2000).
[13] Takeda, E., Todoroki, N., Kitamoto, Y., Abe, M., Inoue, M., Fujii, T., and Arai, K. *J. Appl. Phys.* **87**, 6782 (2000).
[14] Kahl, S. and Grishin, A. *Appl. Phys. Lett.* **84**, 1438 (2004).
[15] Goto, T., Baryshev, A., Tobinaga, K., and Inoue, M. *J. Appl. Phys.* **107**, 09A946 (2010).
[16] Chin, J., Steinle, T., Wehlus, T., Dregely, D., Weiss, T., Belotelov, V., Stritzker, B., and Giessen, H. *Nature Comm.* **4**, 1599 (2013).
[17] Grunin, A., Zhdanov, A., Ezhov, A., Ganshina, E., and Fedyanin, A. *Appl. Phys. Lett.* **97**, 261908 (2010).
[18] Inoue, M., Levy, M., and Baryshev, A., [*Magnetophotonics: From Theory to Applications*], Springer Series in Materials Science (2013).
[19] Inoue, M., Fujikawa, R., Baryshev, A., Khanikaev, A., Lim, P., Uchida, H., Aktsipetrov, O., Fedyanin, A., Murzina, T., and Granovsky, A. *J. Phys. D* **39**, R151 (2006).
[20] Khanikaev, A., Baryshev, A., Inoue, M., and Kivshar, Y. *Appl. Phys. Lett.* **95**, 011101 (2009).
[21] Yeh, P., Yariv, A., and Cho, A. *Appl. Phys. Lett.* **32**, 104 (1978).

[22] Robertson, W. M. and May, M. S. *Appl. Phys. Lett.* **74**, 1800 (1999).
[23] Descrovi, E., Sfez, T., Quaglio, M., Brunazzo, D., Dominici, L., Michelotti, F., Herzig, H., Martin, O., and Giorgis, F. *Nano Lett.* **10**, 2087 (2010).
[24] Soboleva, I., Moskalenko, V., and Fedyanin, A. *Phys. Rev. Lett.* **108**, 123901 (2012).
[25] Guillermain, E., Lysenko, V., and Benyattou, T. *J. Lumin.* **121**, 319 (2006).
[26] Yan, C., Han, L., Yang, J., Gu, W., and Liao, Y. *Sensors and Actuators A* **220**, 85 (2014).
[27] Berreman, D. W. *J. Opt. Soc. Am.* **62**, 502 (1972).
[28] Bethune, D. S. *J. Opt. Soc. Am. B* **8**, 367 (1991).
[29] Romodina, M., Soboleva, I., and Fedyanin, A. *J. Magn. Magn. Mater.* **415**, 82 (2016).
[30] Khanikaev, A., Baryshev, A., Fedyanin, A., Granovsky, A., and Inoue, M. *Opt. Express* **15**, 6612 (2007).